ACS APPLIED MATERIALS & INTERFACES

Research Article

www.acsami.org

Identification of the Chemical Bonding Prompting Adhesion of a-C:H Thin Films on Ferrous Alloy Intermediated by a SiC_x:H *Buffer Layer*

F. Cemin,[†] L. T. Bim,[†] L. M. Leidens,[†] M. Morales,[‡] I. J. R. Baumvol,[§] F. Alvarez,[‡] and C. A. Figueroa*[,†,∥]

[†]Centro de Ciências Exatas e Tecnologia, Universidade de Caxias do Sul, 95070-560 Caxias do Sul, RS, Brazil

[‡]Instituto de Física "Gleb Wataghin", Universidade Estadual de Campinas, 13083-970 Campinas, SP, Brazil

[§]Instituto de Física, Universidade Federal do Rio Grande do Sul, 91509-970 Porto Alegre, RS, Brazil

[∥]Plasmar Tecnologia Ltda., 95030-775 Caxias do Sul, RS, Brazil

ABSTRACT: Amorphous carbon (a-C) and several related materials (DLCs) may have ultralow friction coefficients that can be used for saving-energy applications. However, poor chemical bonding of a-C/DLC films on metallic alloys is expected, due to the stability of carbon−carbon bonds. Silicon-based intermediate layers are employed to enhance the adherence of a-C:H films on ferrous alloys, although the role of such *buffer layers* is not yet fully understood in chemical terms. The chemical bonding of a-C:H thin films on ferrous alloy intermediated by a nanometric SiC_x:H *buffer layer* was analyzed by X-ray photoelectron spectroscopy (XPS). The chemical profile was inspected by glow discharge optical emission spectroscopy (GDOES), and the chemical structure was evaluated by Raman and Fourier transform infrared spectroscopy techniques. The nature of adhesion is discussed by analyzing the chemical bonding at the interfaces of the a-C:H/SiC_x:H/ferrous alloy sandwich structure. The adhesion phenomenon is ascribed to specifically chemical bonding character at the *buffer layer*. Whereas carbon−carbon (C−C) and carbon−silicon (C−Si) bonds are formed at the outermost interface, the innermost interface is constituted mainly by silicon−iron (Si−Fe) bonds. The oxygen presence degrades the adhesion up to totally delaminate the a-C:H thin films. The SiC_x:H deposition temperature determines the type of chemical bonding and the amount of oxygen contained in the *buffer layer*.

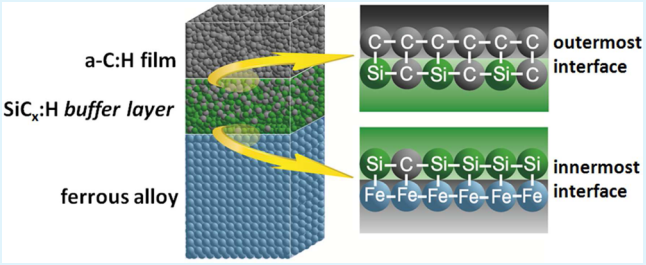

KEYWORDS: *XPS, interface, hydrogenated silicon carbide, hydrogenated amorphous carbon, DLC, adhesion, chemical bonding, buffer layer*

1. INTRODUCTION

Diamond-like carbon (DLC) is a metastable form of amorphous carbon (a-C) that regards a great variety of carbon based thin films.[1] Some varieties of this material have lately attracted much attention due to their properties, such as high wear resistance and superlow friction coefficient.[1,2] However, the poor adhesion of a-C thin films on ferrous alloys is a fact that prevents its technical applications at the industrial scale, in particular, for energy efficiency issues in mechanical devices of engines and vehicles.[1−3]

In order to ensure adherence of a-C thin films on ferrous alloys, many works have reported the use of intermediate layers (from now on *buffer layer*), multilayer coatings, and surface thermochemical treatments previous to the deposition of a-C and related materials.[4−7] These steps aim to create a bonding *buffer layer*, which is particularly beneficial to amend the high intrinsic stress of such thin films by promoting stronger chemical bonds at the interfaces, i.e. a-C:H/SiC_x:H and SiC_x:H/ferrous alloy interfaces, respectively. *Buffer layers* containing silicon are commonly employed for these purposes due to the formation of hard silicon carbide (SiC) compounds containing strong covalent bonds.[8−12] In the attempt to understand the micro-/nanoscale origin and improve the a-C thin films adhesion phenomenon on ferrous alloys, the standard scientific approach to attack the problem follows an exclusively physical point of view, that is, taking into account the momentum transference by the ion bombardment during the deposition process, weak bonds erosion by the ion bombardment, diffusion atoms relocation, local heating spike, and/or different thermal expansion coefficients of a-C and ferrous alloys prompting delamination, spallation, and blistering of films.[3,6] Therefore, the specific chemical bonds, i.e., the affinity of the elements forming the chemical structure of both interfaces, determine the final adhesion behavior, but it is not specifically analyzed in details in order to understand the *buffer layer* role as a sort of "nanoglue". The understanding of the chemical phenomena has an important role on the optimization of DLC adhesion on metallic alloys for tribological applications, where the lifetime of the coating is fundamental for both technical and economic reasons.[13,14]

Received: April 24, 2015
Accepted: July 2, 2015
Published: July 2, 2015

ACS Publications © 2015 American Chemical Society

DOI: 10.1021/acsami.5b03554
ACS Appl. Mater. Interfaces 2015, 7, 15909−15917

Table 1. Process Parameters for Substrate Cleaning and SiC_x:H Buffer Layer and a-C:H Thin Film Depositions in the Samples Thereafter Studied by XPS

	Ar^+ ion cleaning	SiC_x:H *buffer layer*	a-C:H film
Pressure (Pa)	10	60	10
Temp (°C)	~25	100, 300, 500	~80
Time (min)	30	1	1
Precursors (%)	Ar (100)	$Si(CH_3)_4$–Ar (80–20)	C_2H_2–Ar (75–25)
Voltage (V)	−500	−500	−800
Power supply	Pulsed (+30 V) DC, 10 kHz, duty cycle 40%		

Taking into account these considerations, in a previous work, we studied the physicochemical properties of nonstoichiometic hydrogenated silicon carbide (SiC_x:H) *buffer layers* grown from a mixture of tetramethylsilane (TMS) and argon (Ar) by plasma enhanced chemical vapor deposition (PECVD) intercalated between a hydrogenated amorphous carbon (a-C:H) thin film and a ferrous alloy.[15] This work revealed that the adhesion capability of a-C:H thin films on a ferrous alloy depends mainly on the substrate temperature during the *buffer layer* growth. Moreover, the a-C:H does not delaminate for *buffer layers* deposited at temperatures ≥300 °C. We remark that the plasma chemistry of TMS-Ar mixtures and its consequence on the SiC_x:H growth by PECVD were already demonstrated by Soum-Glaude and co-workers.[16,17] In spite of all these efforts, the mechanism of the a-C:H adhesion on ferrous alloys through SiC_x:H *buffer layers* has not been fully understood and a further microscopy scrutiny by XPS analysis of the interfaces local bonding could contribute to elucidate such a mechanism involved in the deposition process.

X-ray photoelectron spectroscopy (XPS) has been used by a few authors to study the chemical bonding at the interfaces of the a-C:H/*buffer layer*/substrate sandwich structure. For instance, Capote and co-workers analyzed the chemical bonding on a silicon *buffer layer* grown from a silane precursor between a titanium alloy (Ti_6Al_4V) and the a-C:H thin film.[8] These authors, however, did not report the details of the bonds involved at the innermost interface, i.e., between the silicon *buffer layer* and the titanium alloy. Regarding the Si–C bonds, Schäfer and co-workers showed, by a XPS study of the first atomic layers of a-C:H deposited on Si(111) wafers, the formation of a very thin (18 Å thick) adhesive layer of SiC.[18] Summarizing, in spite of the experimental evidence about the improved adhesion of a-C:H thin films on pure silicon due to strong Si–C bonds, the mechanism and nature of adhesion from a chemical point of view of a-C:H on ferrous alloys intermediated by Si-based *buffer layers* are not fully understood. Moreover, this is particularly cumbersome on those *buffer layers* grown from TMS, a precursor that does not only contain silicon in the chemical composition, but also carbon and hydrogen.

The aim of this work is to investigate by *in situ* XPS the local chemical bonds at the interfaces of the a-C:H/SiC_x:H/ferrous alloy sandwich structure by sequentially growing the SiC_x:H *buffer layer* and the a-C:H thin film on a ferrous alloy substrate. Also, by a detailed scrutinizing of the interfaces, local chemical bonds evolution as a function of *buffer layer* deposition temperature is carried out in order to identify the main structures responsible for improving the a-C:H adhesion on a ferrous alloy substrate.

2. MATERIALS AND METHODS

The studied bilayers were grown on a low-alloy steel AISI 4140 (composition in wt %: C: 0.40, Cr: 0.96, Mo: 0.17, Si: 0.23, Mn: 0.85, Ni: 0.13, Cu: 0.15 and Fe: balance) by using a pulsed DC-PECVD system assisted by electrostatic plasma confinement.[19] First, the substrates were Ar^+ ion cleaned during 30 min; afterward, the SiC_x:H *buffer layer* was grown from a vapor-gaseous mixture of TMS and Ar during 1 min. The substrate temperatures for the studied samples were fixed at 100 °C, 300 °C, and 500 °C during the SiC_x:H growth. These samples were employed to investigate the local chemical bonding by XPS on the innermost interface of the *buffer layer*, i.e., the SiC_x:H/ferrous alloy interface. In a second group of samples, following the same procedures described above, a thin a-C:H film was grown at 80 °C using a gaseous mixture of acetylene (C_2H_2) and Ar during 1 min on the top of the different studied SiC_x:H layers. These samples were employed to investigate the local chemical bonding by XPS on the outermost interface of the *buffer layer*, i.e., the a-C:H/SiC_x:H interface. Table 1 introduces all the process parameters that were used in the sample preparation and thin film depositions. Complementary information about the deposition system is described elsewhere.[15,19] Only thin layers were grown on the ferrous alloy in order to probe interfaces of interest by the XPS, due to the fact that this technique, as it is well known, can analyze the outermost atomic layers up to ~0.5–2 nm in-depth for the energy of the X-ray used in the experiments.[20]

The chemical composition and bonding of the interfaces were determined by XPS equipment model Thermo Alpha 110 Hemispherical Analyzer using the 1486.6 eV photons from an Al target (K_α line). The binding energy associated with the $3d_{5/2}$ electron energy of Ag is used to determine the equipment Fermi level. The total apparatus resolution is ~0.85 eV (K_α line-width plus analyzer). The pressure in the analysis chamber was $<8 \times 10^{-9}$ mbar during the experiments. A Shirley background subtraction procedure was applied to correct the XPS background spectra stemming from electron inelastic scattering. In order to identify the origin of the bands associated with different photoemitted electrons, a deconvolution procedure was performed by means of the *Thermo Advantage* software. In order to evaluate the chemical bonding at the SiC_x:H/ferrous alloy interface, the SiC_x:H layers grown on the samples of the first group were Ar^+ ion sputtered *in situ* for 2 min before XPS analysis. Similarly, the a-C:H thin films grown on the samples of the second group were Ar^+ ion sputtered *in situ* for 5 min before analysis, in order to inspect the chemical bonding at the a-C:H/SiC_x:H interface. One must remark that in spite of the mixing effect, the chemical structure of both in-depth interfaces remains unchanged due to protection of the outermost layers. In fact, the mixing effect may happen in the outermost atomic layers, but it cannot happen at the interface, i.e., in the underneath atomic layers. This experimental design allows to secure and keeps intact the chemical bonding information at the interface due to the outermost layer deposition protects the interface of the atmosphere contamination.

Moreover, the in-depth chemical profiles were obtained by glow discharge optical emission spectroscopy (GDOES – Horiba GD-Profiler 2). Structural details of the a-C:H thin films and the SiC_x:H *buffer layers* were inspected, respectively, by Raman scattering spectroscopy (Raman Confocal NTegra Spectra NT-MDT (473 nm laser)) and Fourier transform infrared (FTIR) spectroscopy (PerkinElmer FT-IR Spectrometer/model Spectrum 400).

DOI: 10.1021/acsami.5b03554
ACS Appl. Mater. Interfaces 2015, 7, 15909–15917

Finally, nanoscratch tests were carried out in order to quantify the adhesion of thin films by using a nanoindentation system (Micro Materials NanoTest-600), equipped with a conical diamond tip with final radius of 25 μm. A normal load of 0.01 mN was applied in the firsts 100 μm of the scan and then the load was linearly increased at 0.3 mN s^{-1} up to reach a final normal load of 500 mN, as the tip was dragged through a distance of 1,800 μm over the sample surface. The applied normal load to induce failure (delamination) in thin films was considered as the critical load and this value was determined by using both the tangential force data and microscopic observation. The scratch tests were performed in samples where the thickness of the a-C:H thin films was fixed at approximately 1.8 μm.

3. RESULTS AND DISCUSSION

Figure 1 shows a characteristic Raman spectrum of the a-C:H thin film in the a-C:H/*buffer layer*/substrate sandwich

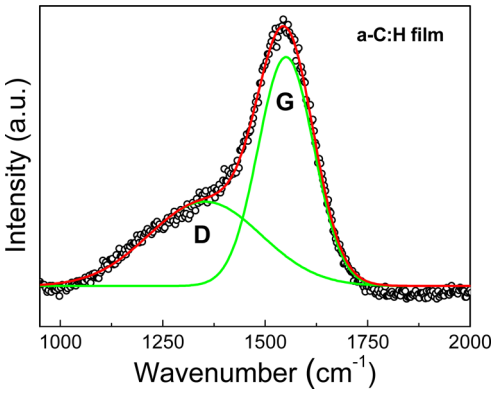

Figure 1. Raman spectrum for the a-C:H thin film deposited on the top of the SiC_x:H *buffer layer* grown at 500 °C.

structure. One can see that the typical disorder (D) and graphitic (G) large bands of the a-C:H structure are apparent at ~1355 and 1550 cm^{-1}, respectively.[1]

Figure 2a shows schematically the in-depth region analyzed by XPS with the purpose to identify the local chemical bonding structure at the innermost interface of the *buffer layer*. *In-situ* Ar^+ sputtering was gradually performed up to the iron concentration 2 at %, i.e., guaranteeing that the SiC_x:H/ferrous alloy interface was effectively reached. Figure 2b and c show, respectively, the Si 2p and the C 1s core electron level photoemission spectra recorded both from the innermost interface (SiC_x:H/ferrous alloy) and the SiC_x:H *buffer layer* grown at variable substrate temperatures. One can notice, also, the chemical shifts of the bands associated with the Si 2p and C 1s electrons toward lower binding energies in samples grown at higher temperatures. This behavior can be attributed to the presence of a more electronegative environment at lower temperatures.

The deconvolution of the bands associated with the Si 2p electrons in the XPS spectra (Figure 2 b) shows the following more probable contributions: Si−Si bonds in pure silicon (Si^0) (~99.5 eV); Si−C bonds (~100.6 eV); O−Si−C bonds (~101.7 eV); and Si−O bonds in SiO_x species (~103 eV).[21,22] The undesired presence of oxygen is due to the oxygen atoms that come from the residual gases absorbed on the deposition chamber walls, such as molecular oxygen (O_2) and vapor water (H_2O). Indeed, a considerable amount of oxygen, varying from 2 to 23%, can be present in a structure of TMS-deposited SiC_x:H films.[22] One can see in Figure 2b a main contribution of silicon bonded to oxygen, as SiO_x and O−

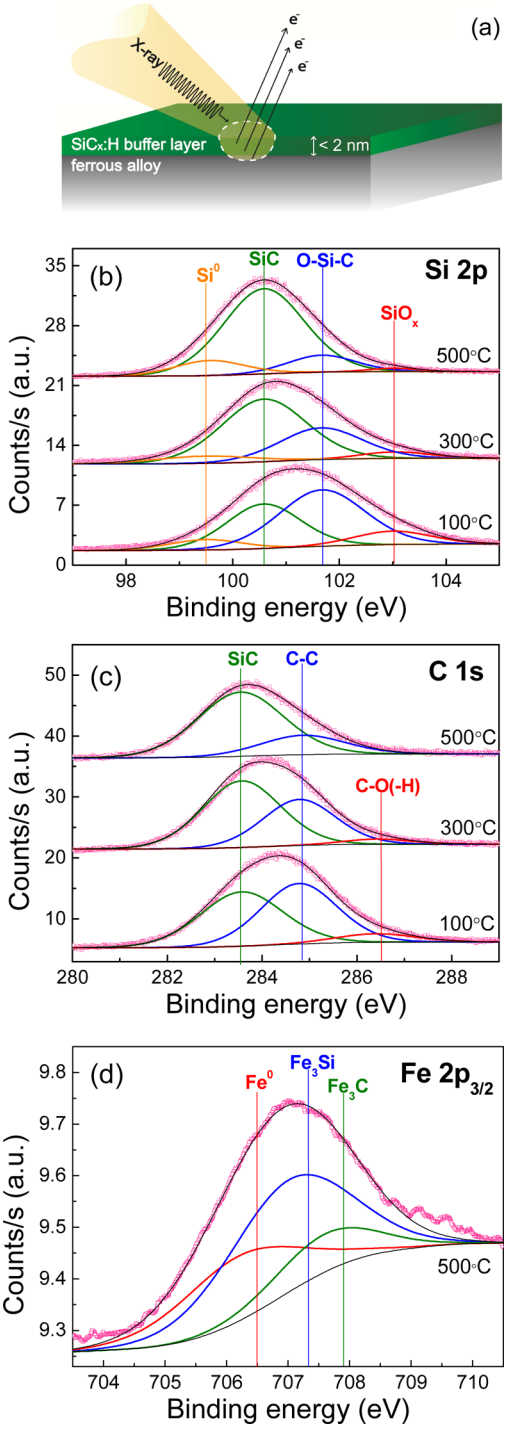

Figure 2. (a) Sketch of the in-depth region analyzed by XPS at the SiC_x:H/ferrous alloy innermost interface; (b), (c), and (d) show, respectively, the bands associated with the Si 2p, C 1s, and Fe $2p_{3/2}$ core electron levels obtained from the photoemission spectra. The proposed spectral deconvolutions are also displayed.

Si−C, when the *buffer layer* is grown at 100 °C. A recent work has shown that Si−O and C−O bonds were detected in Si-DLC multilayers deposited on AISI 304 stainless steel where no external heating was applied and the maximum process temperature was about 180 °C.[23] By increasing the SiC_x:H film deposition temperature up to 500 °C, the Si−O bonds are gradually replaced by Si−C bonds. Concomitantly, the band associated with the O 1s electrons in the XPS spectra revealed a

DOI: 10.1021/acsami.5b03554
ACS Appl. Mater. Interfaces 2015, 7, 15909−15917

decreasing of oxygen content on increasing the SiC_x:H film deposition temperature. Figure 3 shows the oxygen atomic content at variable SiC_x:H film deposition temperatures. One can see that the higher the SiC_x:H film deposition temperature, the lower the oxygen content in the *buffer layer*. Also, the inset shows the relative decrease in the area related to the O 1s electron band at higher SiC_x:H film deposition temperatures. This is so, possibly, due to the fact that oxygen is thermally desorbed at higher temperatures from the growing film surface to the vacuum chamber. As will be shown later, the in-depth oxygen profile in the ferrous alloy is quite similar at variable SiC_x:H film deposition temperature, indicating that oxygen atoms do not diffuse into the substrate. Regarding the SiC content increasing, we note that many authors have reported similar behaviors on growing hydrogenated amorphous silicon carbide (a-SiC:H) and amorphous silicon carbide (a-SiC) films.[16,24−26] These studies show that the increasing of the substrate temperature during the film growth modifies the surface reactivity by increasing the atoms mobility and thus promoting the formation of more stable compounds containing Si−C bonds.[25] It is interesting to note that the Si−C bonds increasing at higher temperature deposition prompts the material densification by favoring reactions leading to decreasing hydrogen and oxygen contents in the SiC_x:H film structure.[24,26] Despite the fact that it is not possible to analyze hydrogen bonded to carbon and silicon atoms in the *buffer layer* structure by XPS, we expect that the hydrogen acts as oxygen, being thermally desorbed at higher temperatures. Indeed, in a previous work, we show that hydrogen content decreases in such *buffer layers* on increasing the deposition temperature.[15]

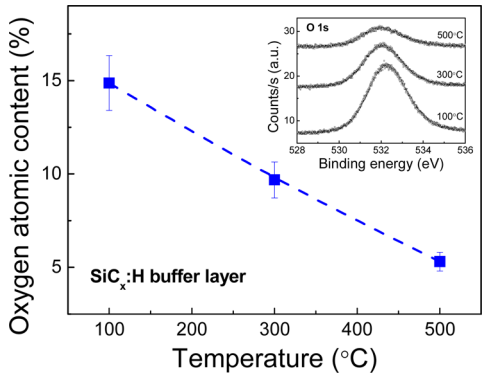

Figure 3. Oxygen atomic content in the SiC_x:H *buffer layer* deposited at different temperatures. Also, the inset shows the bands associated with the O 1s core electron level at different deposition temperatures.

The deconvolution of the band associated with the C 1s electrons in the XPS spectra (Figure 2c) shows the following more probable contributions: Si−C bonds (~283.5 eV), C−C bonds (~284.8 eV), and C−O(−H) bonds (~286.5 eV).[8,21,22] Similarly to the effect observed in the analysis of the band associated with the Si 2p electrons (see Figure 2b), the maximum of the spectrum is shifted to lower binding energies when the SiC_x:H deposition temperature increases from 100 to 500 °C. This chemical shift of the binding energies related to C 1s electrons to lower energies is consistent with the formation of Si−C bonds to the detriment of C−C bonds. We note that the fact of oxygen being more electronegative than both carbon and silicon also explains why the C 1s and Si 2p bands are both shifted to higher binding energies when oxygen is present in the material. According to Figure 3, more oxygen is present at lower SiC_x:H film deposition temperatures.

The same behavior was confirmed by inspecting the SiC_x:H *buffer layer* structure by FTIR. Figure 4 shows the FTIR spectra of the SiC_x:H *buffer layer* deposited at different temperatures. Due to the fact that outgoing infrared radiation could not reach the SiC_x:H/ferrous alloy interface, the FTIR information characterizes the bulk of the SiC_x:H *buffer layer*. One can see that the Si−O−Si asymmetric stretching mode at ~1060 cm^{-1} is the most important contribution for the SiC_x:H *buffer layer* deposited at 100 °C followed by the Si−$(CH_3)_3$ stretching mode at ~840 cm^{-1} and the Si−O−Si, Si−(CH_3), and Si−$(CH_3)_2$ stretching modes at ~790 cm^{-1}.[27,28] Moreover, a sharp peak is observed at ~1263 cm^{-1}, which is related to the Si−$(CH_3)_3$ bending mode where silicon is bonded to oxygen atoms (please, see (O)Si−$(CH_3)_3$ in Figure 4).[27] At higher deposition temperatures, the oxygen contribution decreases and the vibrations are related to oxygen-free Si-$(CH_3)_{1-3}$ structures.

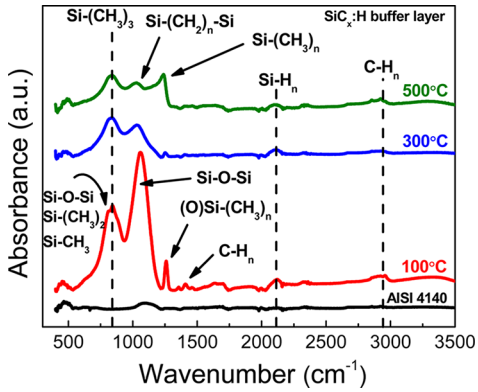

Figure 4. FTIR spectra of the SiC_x:H *buffer layer* deposited at different temperatures.

Figure 2d shows the XPS spectrum associated with the Fe $2p_{3/2}$ core electron level obtained from the SiC_x:H/ferrous alloy interface corresponding to the SiC_x:H grown at 500 °C. The components associated with different bonds obtained after the deconvolution procedure indicated in Figure 2d show the presence of iron and related compounds such as pure iron (Fe^0) (~706.5 eV), iron silicide (Fe_3Si) (~707.3 eV), and iron carbide (Fe_3C) (~707.9 eV).[20] The presence of Fe−O chemical bonds is not expected in the XPS spectra due to the Ar^+ sputtering process before the SiC_x:H layer deposition. The sputtering removal by using Ar^+ plasma is an established procedure to remove native oxides in several materials.[29,30] The dominant presence of Fe_3Si strongly suggests that the adhesion strength of the SiC_x:H *buffer layer* on the ferrous alloy is controlled by Si−Fe bonds (we remark that the same conclusions are drawn from the analysis of the XPS spectra obtained in samples grown at 100 and 300 °C (not shown)). In fact, the preferential formation of Fe_3Si instead of Fe_3C is thermodynamically expected . This is so because the Gibbs free energy of formation is negative for Fe_3Si, ranging from −78.31 kJ mol^{-1} (100 °C) to −77.14 kJ mol^{-1} (500 °C), and positive for Fe_3C, ranging from 18.51 kJ mol^{-1} (100 °C) to 3.59 kJ mol^{-1} (500 °C).[31] Thus, the Fe_3Si formation is a spontaneous process, which possibly explains the small Fe_3C contribution of this compound observed in Figure 2d.

Figure 5 shows the chemical profile obtained by GDOES from the sample with the SiC_x:H *buffer layer* deposited at 300

DOI: 10.1021/acsami.5b03554
ACS Appl. Mater. Interfaces 2015, 7, 15909−15917

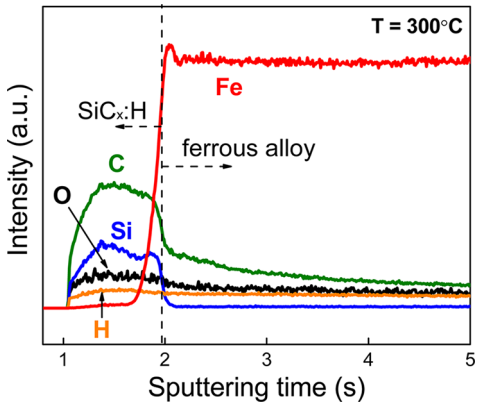

Figure 5. Chemical profile obtained by GDOES for the sample with the SiC_x:H *buffer layer* deposited on the ferrous alloy at 300 °C. System: SiC_x:H/ferrous alloy.

°C on the ferrous alloy after Ar^+ sputtering and XPS analysis. It is clearly seen that there are two different chemical regions. The outermost region is the SiC_x:H *buffer layer*, and the innermost region is the ferrous alloy. As expected from the used precursor, the *buffer layer* is mainly constituted by carbon, silicon, and hydrogen with oxygen as contaminant. In order to analyze further the oxygen profile in both the SiC_x:H and the ferrous alloy, Figure 6 shows the oxygen profiles at different SiC_x:H

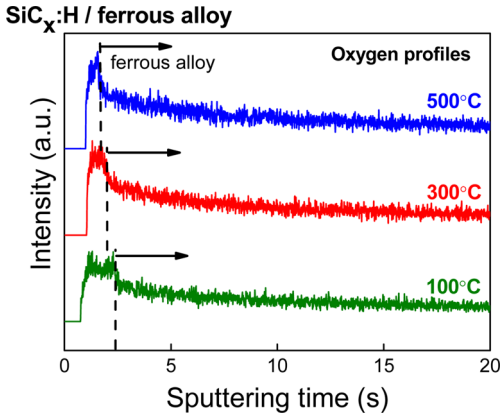

Figure 6. Oxygen profiles obtained by GDOES at different SiC_x:H deposition temperatures. System: SiC_x:H/ferrous alloy.

deposition temperatures. One can see that a higher oxygen signal is apparent at the beginning of the GDOES profiles; that is, a higher oxygen content is measured in the SiC_x:H layer than in the ferrous alloys, independently of the deposition temperature. Moreover, the oxygen signal remains higher for shorter times at higher SiC_x:H deposition temperature due to the *buffer layer* thickness decreasing with the increasing of the deposition temperature.[15] It is important to stress that the in-depth oxygen profile in the ferrous alloy region does not appreciably change at different deposition temperatures, which suggests that oxygen does not diffuse into the bulk material and may be desorbed from the film structure during the growth process at higher deposition temperatures. Consequently, the higher the deposition temperature, the higher the oxygen mobility on the surface, leading to the desorption of oxygen species.

Figure 7a shows schematically the in-depth region analyzed by XPS with the purpose of identifying the local chemical

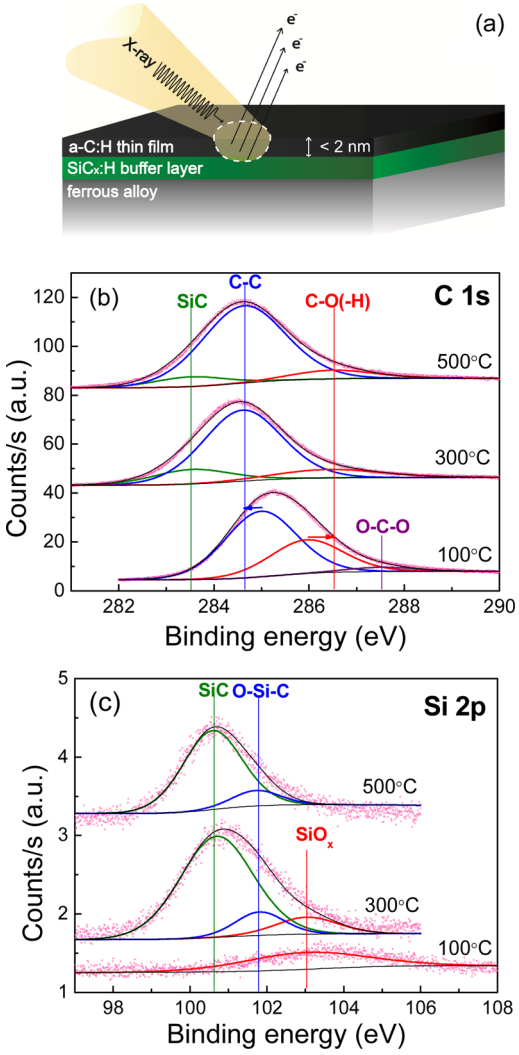

Figure 7. (a) Sketch of the in-depth region analyzed by XPS at the a-C:H/SiC_x:H outermost interface; (b) and (c) show, respectively, the bands associated with the C 1s and Si 2p core electron levels obtained from the photoemission spectra. The proposed spectral deconvolutions are also displayed.

bonding structure at the outermost interface of the *buffer layer*. As explained in the experimental procedure, *in situ* sputtering was performed to obtain a silicon atomic concentration of ~4 at %, guaranteeing that the a-C:H/SiC_x:H interface was reached. Figure 7b and c show, respectively, the bands associated with the C 1s and the Si 2p core electron levels at both the a-C:H thin film and the outermost interface (a-C:H/SiC_x:H) for the *buffer layer* grown at different substrate temperatures.

The components obtained by the deconvolution procedure of the band associated with the C 1s electrons (Figure 7b) are compatible with the presence of Si−C (~283.5 eV), C−C (284.7−285.0 eV), C−O(−H) (~286.0−286.5 eV), and O−C−O bonds (~287.5 eV).[8,21,22] Two different behaviors are observed: on one hand, the band associated with the C 1s electrons shifts to higher binding energies for the SiC_x:H *buffer layer* deposited at 100 °C, strongly suggesting that a large amount of carbon atoms are bonded to oxygen atoms as C−O(−H) and O−C−O; on the other hand, the C 1s band is mainly located at the binding energy compatible with C−C bonds for SiC_x:H *buffer layers* deposited at the temperatures

DOI: 10.1021/acsami.5b03554
ACS Appl. Mater. Interfaces 2015, 7, 15909−15917

ranging from 300 to 500 °C. Moreover, the spectral analysis shows that a smaller amount of carbon atoms are bonded to both oxygen atoms as C−O(−H) and silicon atoms as Si−C in samples obtained at 300 and 500 °C deposition temperatures. The observed Si−C bonds must come from the a-C:H/SiC_x:H interface, which strongly suggests that the adhesion strength of the a-C:H film on the SiC_x:H *buffer layer* is achieved by Si−C bonds through a chemical phenomenon favored at *buffer layer* deposition temperatures of 300 and 500 °C. By referring to C−C and C−O bonds, it is important to emphasize that, at 100 °C deposition temperature, the main peak of the band associated with C−C bonds is slightly shifted to higher binding energies (~285 eV), while the one associated with the C−O(−H) main peak is slightly shifted to lower binding energies (~286 eV), indicating a mixture of these bonds; that is, bonds are not formed exclusively by C−C network atoms but probably also by some intrusive oxygen atoms, as C−C−O structures. The XPS band associated with the O 1s electrons showed lower oxygen content on increasing the SiC_x:H deposition temperature (see Figure 3); that is, oxygen is thermally desorbed from the SiC_x:H structure during the growth process at higher deposition temperatures, as discussed above. Moreover, the FTIR spectra provided a similar behavior where more oxygen is present in the SiC_x:H *buffer layer* deposited at 100 °C (please see Figure 4). According to these results, one can summarize that above 100 °C there are chemical reactions favoring C−O and Si−O bonds dissociation. If this is so, carbon and silicon dangling bonds on the outermost interface of the *buffer layer* are available to bond with carbon atoms, akin to growing a-C:H thin film. Thus, we expect to observe more C−C and Si−C bonds at higher deposition temperatures at such interface, ensuring better adhesion by the formation of more and stronger covalent bonds.

The components obtained from the deconvolution procedure of the band associated with the Si 2p electrons (Figure 7c) are compatible with the presence of Si−C (~100.6 eV), O−Si−C (~101.7 eV), and SiO_x (~103 eV).[21,22] As discussed above in relation to Figure 7b, we have noted two different features in the spectra: on one hand, the Si 2p band is shifted to higher binding energies when the SiC_x:H *buffer layer* is deposited at 100 °C (i.e., the band is located in a position compatible with a binding energy associated with SiO_x species); on the other hand, the band associated with the Si 2p electrons is located at a binding energy corresponding to Si−C bonds when the SiC_x:H *buffer layer* is deposited at different temperatures ranging from 300 to 500 °C, while a lower proportion of silicon atoms are bonded to oxygen atoms. The SiC contribution observed in the band associated with the C 1s core electron level in the XPS spectra (Figure 7b) for the samples deposited at temperatures of 300 and 500 °C is consistent with the results obtained in the Si 2p XPS spectra; that is, the band associated with the later bond is the main contribution in samples deposited at these temperatures. This result strongly suggests that Si−C bonds formed at the outermost interface of the *buffer layer* are involved in the chemical adhesion mechanism of a-C:H thin films on the SiC_x:H *buffer layers* deposited at temperatures ≥300 °C. Thus, for these deposition range of temperatures, C−C bonds and Si−C bonds prompt a better adhesion of a-C:H thin films on the a-C:H/SiC_x:H interface. On the contrary, at lower deposition temperatures (~100 °C), the silicon atoms are mainly bonded to oxygen atoms at the outermost interface of the *buffer layer*, preventing the formation of stronger C−Si bonds. These results are in agreement with the oxygen desorption above-mentioned. At temperatures higher than 100 °C, we suggest that physisorbed oxygen species such as water and molecular oxygen are easily desorbed from the material surface. It is common to observe that the oxygen content in deposited SiC_x:H compounds decreases with the increasing of both temperature and input power of the plasma.[26,32] Moreover, the transition from Si−O to Si−C is not thermodynamically possible because the Gibbs free energy of formation for SiO_2 is more negative than for SiC at either 100 °C (−842.72 kJ mol^{-1} versus −70.24 kJ mol^{-1}) or 500 °C (−770.25 kJ mol^{-1} versus −66.99 kJ mol^{-1}), which supports the oxygen desorption mechanism.[31] Furthermore, it is important to note that hydrogen also might be desorbed from the *buffer layer* structure at higher deposition temperatures, being involved in the chemical adhesion mechanism on the a-C:H/SiC_x:H interface. However, it might be analyzed by GDOES, and more work is necessary before a final conclusion on the subject.

Figure 8 shows the chemical profile obtained by GDOES from the sample with the a-C:H/SiC_x:H/ferrous alloy sandwich

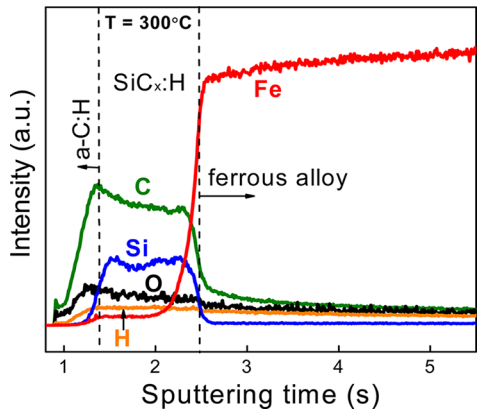

Figure 8. Chemical profile obtained by GDOES for the sample with the a-C:H/SiC_x:H/ferrous alloy sandwich structure and SiC_x:H *buffer layer* deposited on the ferrous alloy at 300 °C.

structure (*buffer layer* deposited at 300 °C) after Ar^+ sputtering and XPS analysis. It is clearly seen that there are three different chemical regions. The outermost region is the remaining a-C:H film, followed by an intermediate SiC_x:H layer, and finally, the innermost region is the ferrous alloy. As expected from the used precursors, the outermost layer is manly constituted by carbon and hydrogen with oxygen as contaminant, followed by silicon, carbon, hydrogen, and, also, oxygen, that form the SiC_x:H *buffer layer*. In order to analyze further the oxygen profile in the a-C:H/SiC_x:H/ferrous alloy sandwich structure, Figure 9 shows the oxygen profiles at different SiC_x:H deposition temperatures. One can see that a higher oxygen signal is apparent at the beginning of the GDOES profiles; that is, a higher oxygen content is measured in both the a-C:H and SiC_x:H layers than in the ferrous alloys, independently of the deposition temperature. Comparing the a-C:H layer to the SiC_x:H layer, the oxygen signal is higher in the a-C:H than in the SiC_x:H at deposition temperatures of 100 and 300 °C, but the oxygen profile is quite similar at 500 °C. Moreover, the oxygen signal decreases with the increasing of the SiC_x:H layer deposition temperature, which is in agreement with the XPS and FTIR results shown in Figures 3 and 4, respectively.

DOI: 10.1021/acsami.5b03554
ACS Appl. Mater. Interfaces 2015, 7, 15909−15917

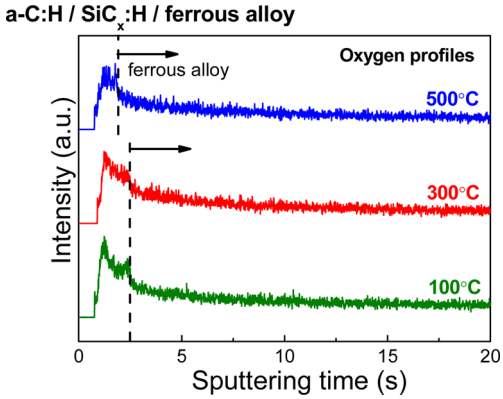

Figure 9. Oxygen profiles obtained by GDOES at different SiC$_x$:H deposition temperatures. System: a-C:H/SiC$_x$:H/ferrous alloy sandwich structure.

Figure 10 shows schematically the atomic structure and bonding of the a-C:H/SiC$_x$:H/ferrous alloy sandwich structure studied by XPS at different deposition temperatures. Growing the *buffer layer* at ~100 °C (see Figure 10a), on one hand, the chemical bonding at the innermost interface (SiC$_x$:H/ferrous alloy) is constituted by Si−Fe. On the other hand, under these low temperature growing conditions, the SiC$_x$:H/a-C:H outermost interface structure presents a large quantity of oxygen atoms bonded to silicon and carbon atoms. As commented above, the oxygen atoms act as terminators of silicon and carbon bonds, preventing the formation of strong C−Si and C−C bonds between carbon atoms belonging to the outermost interface (a-C:H/SiC$_x$:H). Also, zones of likely shear are expected between oxygen terminal atoms from the SiC$_x$:H *buffer layer* and carbon atoms from the a-C:H film, causing very poor practical adhesion and delamination of a-C:H thin films. Table 2 shows the critical load to delaminate the a-C:H thin films from the a-C:H/SiC$_x$:H/ferrous alloy sandwich structure. It is clearly seen that the critical load increases with the increasing of the deposition temperature; that is, higher adhesion is achieved at higher deposition temperature due to the chemical changes introduced at the interfaces. Growing the *buffer layer* at higher temperatures of 300 and 500 °C (see Figure 10b), the chemical bonding at the innermost interface is constituted mainly by Si−Fe and some C−Fe bonds. As discussed above, at these temperatures, residual oxygen atoms are desorbed from the SiC$_x$:H structure, promoting silicon and carbon dangling bonds at the outermost interface and enhancing the chemical affinity between the *buffer layer* and the a-C:H film. Consequently, strong C−C and Si−C covalent bonds are formed at the outermost interface, improving the adhesion of a-C:H thin films on the SiC$_x$:H *buffer layer*.

Finally, we have applied our process in real auto parts in order to illustrate the application of our findings. Figure 11 shows a cylinder liner and a gear after the deposition of the SiC$_x$:H *buffer layer* followed by the a-C:H thin film. The black aspect is due to the presence of adhered a-C:H thin film. In the case of the gear part, the whole piece was coated with the *buffer layer* at ~400 °C and the a-C:H thin film remains on the surface, as expected. In the case of the cylinder liner, the bottom was kept at ~400 °C and the top was intentionally not heated, which leads to a temperature gradient of ~300 °C. Consequently, the top of the cylinder liner shows a massive delamination of the a-C:H thin film where the SiC$_x$:H *buffer layer* is apparent. This last event can be related to a high oxygen content (deposition temperature of ~100 °C) at the outermost interface (a-C:H/SiC$_x$:H) that degrades the chemical adhesion.

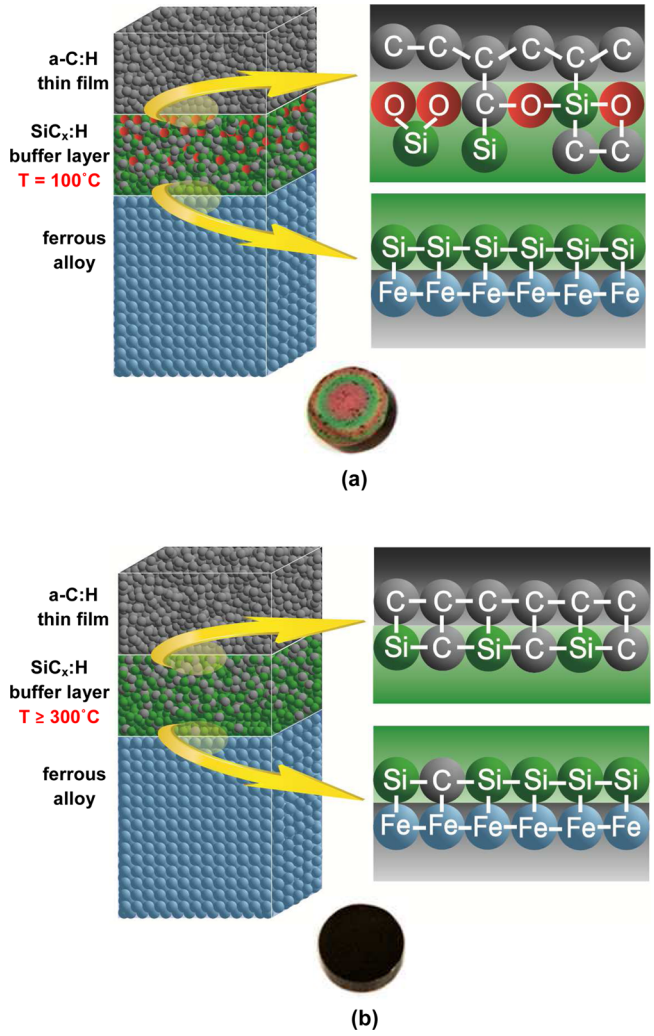

Figure 10. Schematic illustration of the proposed structure and atomic bonding at both interfaces (outermost and innermost) of the SiC$_x$:H *buffer layer* grown at (a) ~100 °C and (b) at ~300 and 500 °C. Also, the top-view photography of samples obtained at 100 and 300 °C is shown below each illustration, respectively. For the sample obtained at 100 °C (a), the a-C:H thin film is totally delaminated and the colors on the surface reveal the SiC$_x$:H *buffer layer*; for the sample obtained at 300 °C (b), one can see a well adhered a-C:H thin film, with critical load for delamination = 298 mN.

Table 2. Critical Load to Delaminate the a-C:H Thin Films (average thickness of 1.8 micrometers) in the a-C:H/SiC$_x$:H/Ferrous Alloy Sandwich Structure Obtained at Different SiC$_x$:H *Buffer Layer* Deposition Temperatures

Temp (°C)	Critical Load (mN)
100	0
300	298 ± 7
500	436 ± 10

4. CONCLUSIONS

In conclusion, the nature of a-C:H thin films adhesion deposited on a ferrous alloy in the presence of a SiC$_x$:H *buffer layer* was studied by XPS in order to identify the local chemical bonding at the interfaces of the a-C:H/SiC$_x$:H/ferrous alloy

DOI: 10.1021/acsami.5b03554
ACS Appl. Mater. Interfaces 2015, 7, 15909−15917

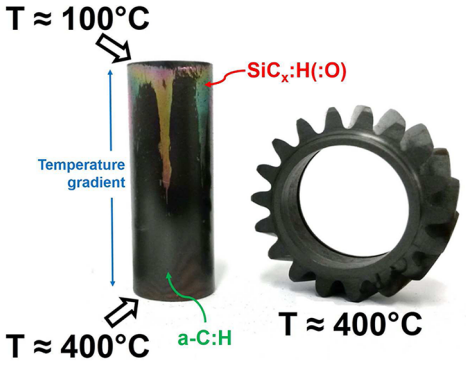

Figure 11. A cylinder liner and a gear after the deposition of the SiC_x:H *buffer layer* followed by the a-C:H thin film. The black aspect is due to the presence of adhered a-C:H thin film. The top of the cylinder liner was intentionally not heated in order to promote a temperature gradient.

sandwich structure. The experimental results show that the chemical bonding at the SiC_x:H/ferrous alloy innermost interface is mainly constituted by Si−Fe for all the studied deposition temperatures for the *buffer layer*. Moreover, at the a-C:H/SiC_x:H outermost interface, the C−C and C−Si bonds are preferentially formed when the *buffer layer* is grown at higher temperatures, namely 300−500 °C range. These findings suggest that the strong covalent bonds at the a-C:H/SiC_x:H outermost interface improve the adhesion of a-C:H thin films. On the contrary, at lower deposition temperatures (~100 °C), carbon and silicon atoms bond to oxygen atoms at the outermost interface; that is, oxygen atoms act as terminators of chemical bonds between the a-C:H thin film and the SiC_x:H *buffer layer*, disrupting the bond network at the outermost interface and jeopardizing the good adhesion of a-C:H thin films. The dominance of this knowledge could be interesting for tailoring the interface chemistry that controls the DLC adhesion on steels by using *buffer layers*, improving the tribological behavior of DLC films deposited on mechanical and electromechanical parts made of ferrous alloys for energy efficiency issues.

AUTHOR INFORMATION

Corresponding Author

*Tel.: +55-54-3218-2764; fax: +55-54-3218-2764; e-mail: cafiguer@ucs.br.

Notes

The authors declare no competing financial interest.

ACKNOWLEDGMENTS

The authors are grateful to UCS, INCT-INES (# 554336/2010-3), CAPES (Brafitec 087/11), PETROBRAS (504062/2014-0), and FAPERGS for financial support. F.C., L.T.B., L.M.L., I.J.R.B., F.A., and C.A.F. are CNPq and CAPES fellows. F.A. is, in part, supported by Fapesp project 2012/10127-5. F.C. is partly supported by PETROBRAS. This work was supported by the SUMA2 Network Project, seventh Framework Program of the European Commission (IRSES Project # 318903). Finally, the authors are grateful to M. E. H. Maia da Costa at PUC-Rio for the Raman spectra.

REFERENCES

(1) Robertson, J. Diamond-Like Amorphous Carbon. *Mater. Sci. Eng., R* **2002**, *37*, 129−281.
(2) Bewilogua, K.; Hofmann, D. History of Diamond-Like Carbon Films − From First Experiments to Worldwide Applications. *Surf. Coat. Technol.* **2014**, *242*, 214−225.
(3) Davis, C. A. A Simple Model for the Formation of Compressive Stress in Thin Films by Ion Bombardment. *Thin Solid Films* **1993**, *226*, 30−34.
(4) Bentzon, M. D.; Mogensen, K.; Hansen, J. B.; Barholm-Hansen, C.; Træholt, C.; Holiday, P.; Eskildsen, S. S. Metallic Interlayers Between Steel and Diamond-Like Carbon. *Surf. Coat. Technol.* **1994**, *68/69*, 651−655.
(5) Wei, C.; Wang, Y.-S.; Tai, F.-C. The Role of Metal Interlayer on Thermal Stress, Film Structure, Wettability and Hydrogen Content for Diamond Like Carbon Films on Different Substrate. *Diamond Relat. Mater.* **2009**, *18*, 407−412.
(6) Wei, C.; Chen, C.-H. The Effect of Thermal and Plastic Mismatch on Stress Distribution in Diamond Like Carbon Film under Different Interlayer/Substrate System. *Diamond Relat. Mater.* **2008**, *17*, 1534−1540.
(7) Silva, V. M.; Carneiro, J. R.; Trava-Airoldi, V. J. Effect of Carbonitriding Temperature Process on the Adhesion Properties of Diamond Like-Carbon Coatings Deposited by PECVD on Austenitic Stainless Steel. *Diamond Relat. Mater.* **2014**, *42*, 58−63.
(8) Capote, G.; Bonetti, L. F.; Santos, L. V.; Trava-Airoldi, V. J.; Corat, E. J. Adherent Amorphous Hydrogenated Carbon Films on Metals Deposited by Plasma Enhanced Chemical Vapor Deposition. *Thin Solid Films* **2008**, *516*, 4011−4017.
(9) Jun, Y.; Choi, J.-Y.; Lee, K.-R.; Jeong, B.-K.; Kwon, S.-K.; Hwang, C.-H. Application of Diamond-Like Carbon Films to Spacer Tools for Electron Guns of Cathode Ray Tube (CRT). *Thin Solid Films* **2000**, *377−378*, 233−238.
(10) Michler, T.; Grischke, M.; Traus, I.; Bewilogua, K.; Dimigen, H. DLC Films Deposited by Bipolar Pulsed DC PACVD. *Diamond Relat. Mater.* **1998**, *7*, 459−462.
(11) Xie, Z.-H.; Singh, R.; Bendavid, A.; Martin, P. J.; Munroe, P. R.; Hoffman, M. Contact Damage Evolution in a Diamond-Like Carbon (DLC) Coating on a Stainless Steel Substrate. *Thin Solid Films* **2007**, *515*, 3196−3201.
(12) Erdemir, A.; Eryilmaz, O. L.; Nilufer, I. B.; Fenske, G. R. Effect of Source Gas Chemistry on Tribological Performance of Diamond-Like Carbon Films. *Diamond Relat. Mater.* **2000**, *9*, 632−637.
(13) Erdemir, A.; Erilymaz, O. Achieving Superlubricity in DLC Films by Controlling Bulk, Surface, and Tribochemistry. *Friction* **2014**, *2*, 140−155.
(14) Holmberg, K.; Andersson, P.; Erdemir, A. Global Energy Consumption Due to Friction in Passenger Cars. *Tribol. Int.* **2012**, *47*, 221−234.
(15) Cemin, F.; Bim, L. T.; Menezes, C. M.; Aguzzoli, C.; Maia da Costa, M. E. H.; Baumvol, I. J. R.; Alvarez, F.; Figueroa, C. A. On the Hydrogenated Silicon Carbide (SiC_x:H) Interlayer Properties Prompting Adhesion of Hydrogenated Amorphous Carbon (a-C:H) Deposited on Steel. *Vacuum* **2014**, *109*, 180−183.
(16) Soum-Glaude, A.; Thomas, L.; Tomasella, E. Amorphous Silicon Carbide Coatings Grown by Low Frequency PACVD: Structural and Mechanical Description. *Surf. Coat. Technol.* **2006**, *200*, 6425−6429.
(17) Soum-Glaude, A.; Thomas, L.; Dollet, A.; Ségur, P.; Bordage, M. C. Argon/Tetramethysilane PECVD: From Process Diagnostic and Modeling to a-Si:C:H Hard Coating Composition. *Diamond Relat. Mater.* **2007**, *16*, 1259−1263.
(18) Schäfer, J.; Ristein, J.; Miyazaki, S.; Ley, L. Formation of the Interface between c-Si(111) and Diamond-Like Carbon Studied with Photoelectron Spectroscopy. *Appl. Surf. Sci.* **1998**, *123/124*, 11−16.
(19) Corujeira Gallo, S.; Crespi, A. E.; Cemin, F.; Figueroa, C. A.; Baumvol, I. J. R. Electrostatically Confined Plasma in Segmented Hollow Cathode Geometries for Surface Engineering. *IEEE Trans. Plasma Sci.* **2011**, *39*, 3028−3032.
(20) Briggs, D.; Seah, M. P. *Practical Surface Analysis*, 2nd ed; John Wiley & Sons: Chichester, 1993.

DOI: 10.1021/acsami.5b03554
ACS Appl. Mater. Interfaces 2015, 7, 15909−15917

(21) Moulder, J. F.; Stickle, W. F.; Sobol, P. E.; Bomben, K. D. *Handbook of X-ray Photoelectron Spectroscopy*; Perkin-Elmer Corp., Physical Electronics Division: MN, 1992.
(22) Choi, W. K. In *Silicon-Based Materials and Devices*; Nalwa, H. S., Ed.; Academic Press: Burlington, 2001; Chapter 1, pp 2−71.
(23) Wang, J.; Pu, J.; Zhang, G.; Wang, L. Interface Architecture for Superthick Carbon-Based Films toward Low Internal Stress and Ultrahigh Load-Bearing Capacity. *ACS Appl. Mater. Interfaces* **2013**, *5*, 5015−5024.
(24) Bayne, M. A.; Kurokawa, Z.; Okorie, N. U.; Roe, B. D.; Johnson, L.; Moss, R. W. Microhardness and Other Properties of Hydrogenated Amorphous Silicon Carbide Thin Films Formed by Plasma-Enhanced Chemical Vapor Deposition. *Thin Solid Films* **1983**, *107*, 201−206.
(25) El Khakani, M. A.; Chaker, M.; O'Hern, M. E.; Oliver, W. C. Linear Dependence of Both the Hardness and the Elastic Modulus of Pulsed Laser Deposited a-SiC Films upon Their Si−C Bond Density. *J. Appl. Phys.* **1997**, *82*, 4310−4318.
(26) Ivashchenko, V. I.; Dub, S. N.; Porada, O. K.; Ivashchenko, L. A.; Skrynskyy, P. L.; Stegniy, A. I. Mechanical Properties of PECVD a-SiC:H Thin Films Prepared from Methyltrichlorosilane. *Surf. Coat. Technol.* **2006**, *200*, 6533−6537.
(27) Grill, A.; Neumayer, D. A. Structure of Low Dielectric Constant to Extreme Low Dielectric Constant SiCOH Films: Fourier Transform Infrared Spectroscopy Characterization. *J. Appl. Phys.* **2003**, *94*, 6697−6707.
(28) Szeto, R.; Hess, D. W. Correlation of Chemical and Electrical Properties of Plasma-Deposited Tetramethylsilane Films. *J. Appl. Phys.* **1981**, *52*, 903−908.
(29) Wang, A.; Ohashi, O.; Yamaguchi, N.; Aoki, M.; Higashi, Y.; Hitomi, N. Cleaning of Diffusion Bonding Surface by Argon Ion Bombardment Treatment. *Nucl. Instrum. Methods Phys. Res., Sect. B* **2003**, *206*, 219−223.
(30) Peters, A. M.; Nastasi, M. Plasma Immersion Ion Cleaning of Oxidized Steel Surfaces Using Hexafluoroethane and Argon Plasmas. *J. Vac. Sci. Technol., A* **2001**, *19*, 2773−2778.
(31) Barin, I. *Thermochemical Data of Pure Substances*; VCH: Weinheim, 1989.
(32) Catherine, Y.; Zamouche, A. Glow Discharge Deposition of Tetramethylsilane Films. *Plasma Chem. Plasma Process.* **1985**, *5*, 353−368.

DOI: 10.1021/acsami.5b03554
ACS Appl. Mater. Interfaces 2015, 7, 15909−15917